

SIMULATIONS OF POSITRON INJECTOR FOR Ce⁺BAF*

A. Ushakov^{†,1}, J. Benesch¹, J. Grames¹, V. Lizárraga-Rubio², S. Ogur¹, R. Rimmer¹, Y. Roblin¹, D. Turner¹, E. Voutier³, S. Wang¹

¹Thomas Jefferson National Accelerator Facility, Newport News, VA, USA

²University of Guanajuato, León, Mexico

³Paris-Saclay University, CNRS/IN2P3/IJCLab, Orsay, France

Abstract

A baseline concept for a continuous wave (CW) polarized positron injector was developed for the Continuous Electron Beam Accelerator Facility (CEBAF) at Jefferson Lab. This concept is based on the generation of CW longitudinally polarized positrons by a high-current, polarized electron beam (1 mA, 130 – 370 MeV, and 90% longitudinal polarization) that passes through a rotating, water-cooled, tungsten target. The simulation results for the Ce⁺BAF injector at the Low Energy Recirculator Facility (LERF) are presented, including positron beam generation, capture, energy selection, and acceleration to 123 MeV. The positron yield (or positron current) and longitudinal polarization are calculated considering the longitudinal and transverse CEBAF acceptances (<1% energy spread, 1.2 mm bunch length and normalized emittance of 100 mm·mrad). The impact of target thickness, drive electron beam energy, and transverse size on positron yield within the required emittance limit is evaluated.

INTRODUCTION

A conceptual design for Ce⁺BAF 12 GeV beginning with a new e⁺ injector at the LERF and ending with injection into CEBAF was developed in 2023 [1,2]. The positron production and polarization transfer from a CW longitudinally polarized electron beam to positrons via bremsstrahlung radiation and e⁺e⁻-pair production in a high-Z conversion target, referred as the PEPPo (Polarized Electrons for Polarized Positrons) technique [3], has been adopted to generate positrons. The e⁺ injector design includes a conversion target, a capture system (based on a focusing solenoid and normal conducting CW capture cavities), an energy selection chicane, an SRF linac, and a bunch compression chicane. This design met the CEBAF physics required positron intensity and polarization requirements (>50 nA with >60% polarization, and >1 μA with low polarization). While the skeleton design was functionally sound, it was built from idealized magnetic and radio-frequency cavity components [2]. To develop the second-generation e⁺ injector design, start-to-end tracking simulations were performed. The design incorporates detailed absorber and solenoid models at the target [4], as well as a realistic model of an normal-conducting

capture cavity [5]. It also uses CEBAF-style beamline magnets and an SRF cryomodule.

The first-generation injector design met CEBAF's requirements for longitudinal acceptance, with an rms momentum spread <1% and a bunch length <1.2 mm [2]. However, the normalized emittance of about 1500 mm·mrad at the end of the 123 MeV e⁺ injector significantly exceeded the CEBAF emittance limit of 100 mm·mrad. The e⁺ yield (or current) of the updated injector design was calculated within the required emittance limit for a highly polarized mode (>60% longitudinal polarization) with a drive electron beam energy of 130 MeV. The evolution of main e⁺ beam parameters along the injector beamline is presented in this paper. The first evaluations aimed at reducing emittance without penalizing the final e⁺ beam current. These studies explored the e⁺ yield for different transverse sizes of the electron beam at the target, as well as for different target thicknesses and electron beam energies.

POSITRON INJECTOR MODEL AND SIMULATION RESULTS

The elegant code [6] was used to design a e⁺ injector layout and calculate beam parameters. Figure 1 shows a schematic layout of the e⁺ injector. The following abbreviations are used for injector components: bucking solenoid (BS), conversion target (T), solenoids of capture system (S1, S2), shielding (SH), normal conducting capture cavity (NC RF), matching sections (MS1, MS2), dipoles (D1–D4), beam collimators (C1–C5), CEBAF superconducting module C75 (SRF Module).

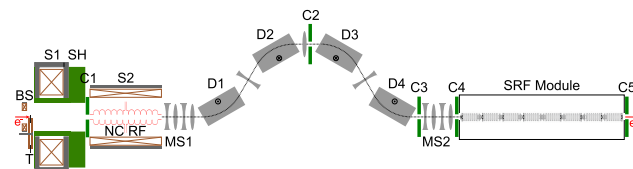


Figure 1: Schematic layout of positron injector.

The electron drive beam used in the simulations below assumes a current of 1 mA at 130 MeV, 90% longitudinal polarization and transverse RMS beam size of 1 mm. The development of an electron source with such a high current and a charge lifetime exceeding 1000 Coulombs is ongoing [7] and it is conducted under a Laboratory Directed Research and Development (LDRD) Program at the JLab. Geant4 [8, 9] has been used to calculate the positron conversion in a 4 mm thick tungsten target. Geant4 data at the

* Work supported by the U.S. Department of Energy, Office of Science, Office of Nuclear Physics under contract DE-AC05-06OR23177. The research described in this paper was conducted under the Laboratory Directed Research and Development Program at Thomas Jefferson National Accelerator Facility for the U.S. Department of Energy.

† ushakov@jlab.org

target exit was used for tracking through the whole injector in elegant. The tungsten of 4 mm thickness was the optimal thickness for the figure-of-merit, which is defined as the product of yield and square of longitudinal polarization, for 120 MeV electron beam and capture of 60 MeV e^+ at the target exit [10]. A 3D magnetic field of the BS and S1 solenoids was imported into elegant. Similar to the previous studies [4], the solenoid S1 has a 20 cm inner radius, but the coil length was reduced to 40.8 cm. The S1 iron core has a thickness of 16.5 cm. The peak strength of S1 on the beam axis was 1.6 T. To reduce the loss of 60 MeV positrons in the standing wave CW capture cavity (1497 MHz, 4 MV/m, 11 cells with an iris radius of 4 cm [5]), the strength of the S2 solenoid was increased to 0.9 T. The bending angle of dipoles in the momentum selection chicane is 0.204 rad, which is the same as in the first-generation injector model. The CEBAF cryomodule C75, which has a total length of 8 m and 8 cavities with 7 cells and a 2.65 cm iris radius, was used to accelerate positrons to 123 MeV. The apertures of the circular collimators (C1 and C4/C5) are equal to the radius of the cavities (NC RF and SRF). The X-half aperture of rectangular collimators C2 and C3 is 1.5 cm. The half-gap between dipole poles and radius of beam pipe is 5 cm.

The current model does not include a bunch compression chicane because the compression can be achieved in the transport line downstream of the injector. The results of beam tracking through the positron transport line from the injector at LERF to the injection point in the north linac, as well as tracking through the 12 GeV Ce⁺BAF up to the experimental halls, are presented at this conference [11].

The average e^+ momentum and the momentum spread along the beam path are shown in Fig. 2. RMS spread is reduced from 96% at the target exit ($s = 0$) to 0.76% at the end of injector. The e^+ capture and energy selection systems were optimized to minimize the losses of 60 MeV e^+ at the target exit. The e^+ yield is reduced from $2.5 \cdot 10^{-1} e^+/e^-$ at the target exit to $3.5 \cdot 10^{-4} e^+/e^-$ at the SRF module exit, as shown in Fig. 3. The change of bunch length along the injector is also shown in this figure. The longitudinal RMS size of the bunch at the end of injector is 3.5 mm.

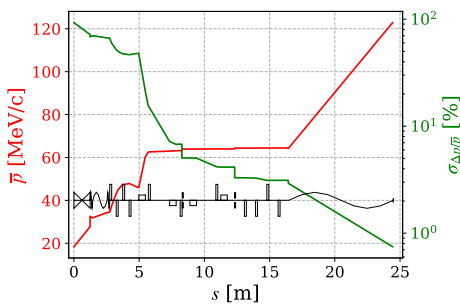


Figure 2: Average positron momentum and RMS momentum spread along injector beamline.

The RMS transverse beam sizes and angles are shown in Fig. 4 and 5, respectively. The positron beam at the end of the

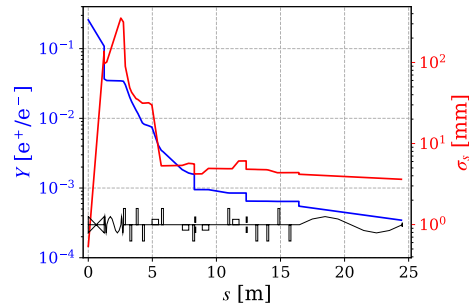


Figure 3: Positron yield and bunch length versus s .

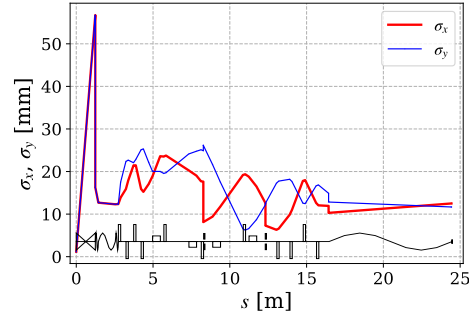


Figure 4: Transverse RMS beam sizes versus s .

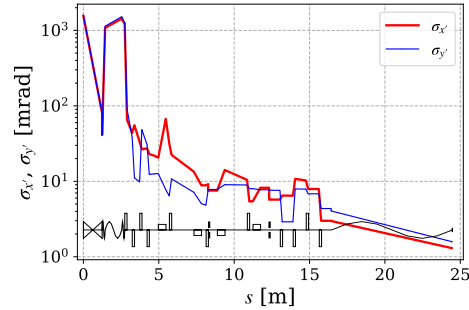
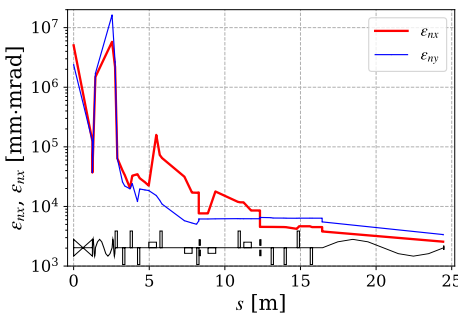
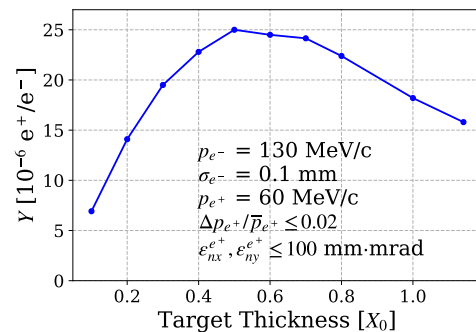
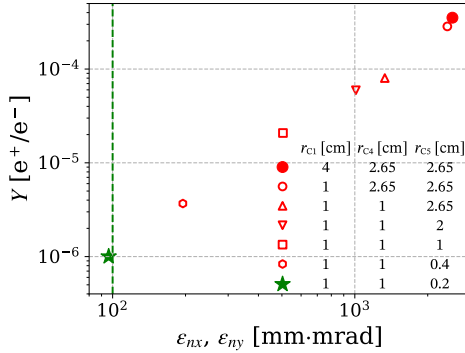


Figure 5: Beam divergence angles (RMS) versus s .

injector has an RMS beam size of 12 mm and a divergence angle of about 1.5 mrad.

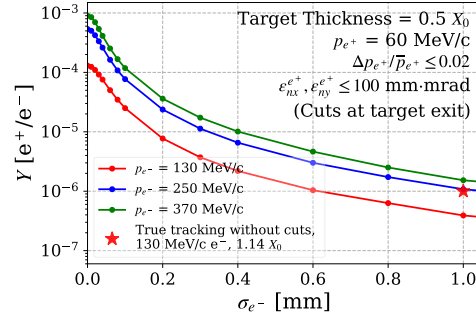
The evolution of normalized emittances ε_{nx} and ε_{ny} along the beam line is shown in Fig. 6. The normalized emittances, starting with $\gtrsim 2 \cdot 10^6$ mm·mrad at the target due to high divergence angles of > 1000 mrad, are reduced to ε_{nx} of $2.6 \cdot 10^3$ mm·mrad and ε_{ny} of $3.3 \cdot 10^3$ mm·mrad at the end of the injector. The difference of ε_{nx} and ε_{ny} is caused by the difference in x and y half-widths of C2 and C3. The collimator C2, which is located right before the capture cavity, and the collimators C4 and C5, which are positioned before and after the SRF module, are used to reduce the emittance to 100 mm·mrad. Figure 7 shows the values of e^+ yield and emittance for the different collimators. The red solid circle (top-right) in this figure corresponds to the collimators used in Figs. 2-6. The reduction of normalized emittance to 100 mm·mrad reduces the yield to $1 \cdot 10^{-6} e^+/e^-$. In the following section, we aim to explore possibilities for increasing e^+ yield while maintaining the required emittance level.

Figure 6: Normalized x and y emittances versus s .Figure 8: e^+ yield versus target thickness.Figure 7: Yield versus normalized emittance. Rectangular collimators C2 and C3 have half aperture in x direction of 1.5 cm; green line is max emittance accepted by CEBAF.

IMPACT OF TARGET THICKNESS, e^- BEAM SIZE AND ENERGY ON e^+ YIELD

A parametric study was started to evaluate what modifications could be made to reduce emittance without reducing e^+ yield too much. The parameters that were selected for the study included the target thickness, the e^- beam energy, and the e^- beam spot size on the target. For each parameter, the e^+ yield was calculated within a normalized emittance of less than 100 mm·mrad, a momentum of 60 MeV/ c , and a momentum spread of less than 2% at the target exit. The yield was calculated in Geant4 at the exit side of the tungsten target. The target thickness was varied between 0.1 X_0 and 1.14 X_0 , where X_0 is the radiation length (3.5 mm for tungsten). The e^- beam size was varied between 0.1 mm and 1 mm (RMS). The values of the e^- beam energy are defined by the energy of the polarized e^- pre-accelerator (10 MeV) and the energy gained in two SRF C75 cryomodules (2×60 MeV): 100 MeV for a single pass, 250 MeV after the first recirculation, and 370 MeV after the second recirculations. In these simulations, the e^- beam energy spread, divergence, and bunch length were purposely fixed at zero to eliminate their dependencies. Figure 8 illustrates the influence of target thickness on the yield for a 130 MeV e^- beam with a 0.1 mm RMS beam size. A reduction of the target thickness from 1.14 X_0 to 0.5 X_0 increases the e^+ yield by 55% and reduces the heat induced by beam in the target by a factor of 3.2.

The transverse size of the e^- beam has a strong impact on the e^+ yield, as shown in Fig. 9. Decreasing the RMS spot size from 1 mm to 0.1 mm reduces the emittance by a factor of 63, 71, and 77 for electron beams of 130, 250, and 370 MeV, respectively. Increasing e^- energy from 130 to 370 MeV for the same target thickness increases the e^+ yield by a factor of ≈ 5 .

Figure 9: e^+ yield versus e^- beam size.

The e^+ yield calculated at the target exit by applying emittance and momentum cuts (red curve in Fig. 9) is lower by a factor > 2.5 in comparison to the yield obtained from the start-to-end beam tracking (red star) for a 130 MeV e^- beam. To make the fast e^+ yield evaluations, the momentum spread at the target exit can be increased from 2% to 5%. To calculate the e^+ yield with a good accuracy, the positrons must be tracked through the injector model.

SUMMARY

A model of the positron injector has been updated, and realistic geometries and field maps of the capture solenoids and cavity have been included. The e^+ beam has been tracked through the model of the injector for the high polarization mode with a drive e^- beam of 130 MeV and a tungsten target of 4 mm thickness. It was found that a normalized emittance at the end of the injector can be reduced to 100 mm·mrad by selecting the proper collimators. The resulting yield is low ($\approx 1 \cdot 10^{-6} e^+/e^-$) and should be increased. We are exploring how the e^+ yield depends on target thickness, e^- beam size and e^- energy to define the best target thickness and smallest electron beam size and to provide the highest possible currents to the experimental halls.

REFERENCES

- [1] J. Grames *et al.*, “Positron beams at Ce⁺BAF”, in *Proc. IPAC’23*, Venice, Italy, May 2023, paper MOPL152, pp. 896–899. doi:10.18429/JACoW-IPAC2023-MOPL152
- [2] S. Habet, “Concept of a polarized positron source for CE-BAF”, Ph.D. thesis, Paris-Saclay University, France, Dec. 2023. <https://theses.hal.science/tel-04584936>
- [3] D. Abbott *et al.*, “Production of highly polarized positrons using polarized electrons at MeV energies”, *Phys. Rev. Lett.*, vol. 116, p. 214801, May 2016. doi:10.1103/PhysRevLett.116.214801
- [4] A. Ushakov *et al.*, “Simulations of positron capture at Ce⁺BAF”, in *Proc. IPAC’24*, Nashville, TN, USA, May 2024, paper MOPC54, pp. 184–187. doi:10.18429/JACoW-IPAC2024-MOPC54
- [5] S. Wang *et al.*, “Capture cavities for the CW polarized positron source Ce⁺BAF”, in *Proc. IPAC’24*, Nashville, TN, USA, May 2024, paper MOPC51, pp. 173–175. doi:10.18429/JACoW-IPAC2024-MOPC51
- [6] M. Borland, “elegant: A flexible SDDS-compliant code for accelerator simulation”, Argonne National Lab, IL, USA, Rep. LS-287, Aug. 2000. doi:10.2172/761286
- [7] M. Bruker *et al.*, “Toward a long-lifetime polarized photoelectron gun for the Ce⁺BAF positron source”, in *Proc. IPAC’24*, Nashville, TN, USA, May 2024, paper MOPC52, pp. 176–179. doi:10.18429/JACoW-IPAC2024-MOPC52
- [8] J. Allison *et al.*, “Recent developments in Geant4”, *Nucl. Instrum. Methods Phys. Res. A*, vol. 835, pp. 186–225, 2016. doi:10.1016/j.nima.2016.06.125
- [9] S. Agostinelli *et al.*, “Geant4 – a simulation toolkit”, *Nucl. Instrum. Methods Phys. Res. A*, vol. 506, pp. 250–303, 2003. doi:10.1016/S0168-9002(03)01368-8
- [10] S. Habet, A. Ushakov, and E. Voutier, “Characterization and optimization of polarized and unpolarized positron production”, Tech. Rep. PEPPo TN-23-01, JLAB-ACC-23-3794, Feb. 2023. doi:10.48550/arXiv.2401.04484
- [11] S. Ogur *et al.*, “Transport of 12 GeV positron beams at Ce⁺BAF”, presented at NAPAC’25, Sacramento, CA, USA, Aug. 2025, paper THP056, this conference.